

# Generation of bases and anions from inorganic and organometallic photoinitiators<sup>☆</sup>

Charles Kutal \*

*Department of Chemistry, University of Georgia, Athens, GA 30602, USA*

Received 14 September 1999; accepted 10 January 2000

## Contents

|   |     |
|---|-----|
| Abstract . . . . .                            | 353 |
| 1. Introduction . . . . .                     | 354 |
| 2. Base-generating photoinitiators . . . . .  | 355 |
| 3. Anion-generating photoinitiators . . . . . | 361 |
| 4. Concluding remarks . . . . .               | 367 |
| Acknowledgements . . . . .                    | 367 |
| References . . . . .                          | 367 |

## Abstract

Photosensitive materials composed of a substrate (monomer, oligomer or polymer) and a photoinitiator play a central role in numerous commercial processes. Most photoinitiators in common use are organic compounds that, upon irradiation, produce radicals and/or acids. The desire to expand the scope of photoinitiated chemistry has led to the recent discovery of several classes of inorganic and organometallic photoinitiators that photochemically release neutral Lewis bases and/or anions. This article provides an overview of the author's research program to develop novel photobase and photoanion generators. Fundamental studies of these systems and examples of their potential applications are described. © 2001 Elsevier Science B.V. All rights reserved.

**Keywords:** Photoinitiator; Photoinitiation; Photobase generation; Photoanion generation

<sup>☆</sup> Dedicated to Arthur W. Adamson, an outstanding scientist and mentor, on the occasion of his 80th birthday.

\* Tel.: +1-706-5422035; fax: +1-706-5429454.

E-mail address: [ckutal@sunchem.chem.uga.edu](mailto:ckutal@sunchem.chem.uga.edu) (C. Kutal).

## 1. Introduction

Photoinitiated reactions of monomers, oligomers, and polymers (the substrate) form the basis of several commercially-important technologies such as the photocuring of coatings, adhesives, and inks, the lithographic imaging of electronic components and printing plates, and the production of holograms and optical waveguides [1,2]. While the details of the chemistry will vary depending upon the constituents of the system, the essential features of the photoinitiation process can be described by a two-step sequence. Absorption of a photon by the photoinitiator, PI, causes a photochemical reaction that produces one or more reactive species, IN (Eq. (1)). Subsequent thermal reaction of IN with the substrate results in product formation (Eq. (2)). Several roles can be envisioned for IN in this second step. For example, IN may be consumed while undergoing a



stoichiometric reaction with the substrate. Since at least one photon is required per product molecule formed, the quantum efficiency of product formation (moles of product/moles of absorbed photons) does not exceed unity. Alternatively, IN may serve as a true catalyst and suffer no permanent change in chemical composition in the product forming step (Eq. (3)). Finally, IN may be consumed while initiating a chain reaction such as polymerization (Eq. (4)). In each of the latter two cases, the action of a single photon generates an IN species that results in the conversion of several substrate molecules to product. This chemical amplification of the original photochemical act can result in an effective quantum efficiency considerably greater than unity, thus allowing the design of systems exhibiting high photosensitivity.



Photoinitiated reactions offer several potential advantages over conventional thermally-activated processes. Absorption of a photon by PI (Eq. (1)) generates an electronic excited state whose chemical reactivity can differ substantially from that of the ground state. Consequently, the involvement of an excited state may introduce a reaction pathway that does not occur thermally or occurs only at inconveniently high temperatures. Regulation of light intensity affords a convenient means of controlling reaction kinetics, while the use of patterned light permits exquisite spatial definition of the reaction zone. Other potential advantages of photochemical reactions include reduced energy requirements, increased shelf life of substrate formulations, and greater compatibility with heat-sensitive materials.

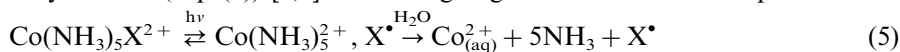
While the optimal properties of a photoinitiator often are dictated by the intended application, we can identify several desirable features that all practical photoinitiators should possess. These include:

1. strong absorption at wavelengths characteristic of the photoexcitation source,
2. thermal stability in the presence of other system components,
3. high quantum efficiency ( $> 0.1$ ) of IN production and/or high chemical amplification,
4. ease of synthesis and modest cost,
5. low toxicity and environmental impact.

For the vast majority of reported photoinitiators, IN is a radical or a strong acid [3–6]. Common radical-generating photoinitiators include benzoin and its derivatives, benzil ketals, substituted acetophenones, aromatic ketone/amine combinations, acylphosphine oxides, dye–borate systems, and fluorinated titanocene derivatives. Among the more popular acid-generating photoinitiators are 2-nitrobenzyl esters, triazines, cationic iron(II)-sandwich complexes, and onium salts belonging to the diaryliodonium and triarylsulfonium families. Studies conducted in the author's laboratory over the past decade have been designed to expand the available selection of photoinitiators to include inorganic and organometallic complexes that undergo photochemical release of uncharged Lewis bases and/or anions. Our primary goals have been to demonstrate the feasibility and generality of photobase- and photoanion-initiated reactions, to elucidate the mechanisms by which these reactions occur, and to develop novel photosensitive materials based upon this chemistry. Succeeding sections of this article will review our progress in this exciting new area lying at the interface of photochemistry and materials science.

## 2. Base-generating photoinitiators

Uncharged nitrogen bases such as ammonia, alkylamines, and pyridine coordinate to transition metals via their lone-pair electrons. Since coordination masks the basic properties of these molecules, the resulting metal complexes can serve as latent sources of photogenerated base. Exemplary in this regard are acidopentaamminecobalt(III) complexes of general formula  $\text{Co}(\text{NH}_3)_5\text{X}^{2+}$ , where  $\text{X}^-$  is a uninegative ligand such as  $\text{Cl}^-$ ,  $\text{Br}^-$ , or  $\text{NCS}^-$ . Typically, these low-spin  $d^6$  complexes are easily synthesized, thermally inert, and strongly absorbing in the ultraviolet wavelength region owing to the presence of X-to-Co charge transfer excited states. Populating these ligand-to-metal charge transfer states creates a labile Co(II) center that, in solution, undergoes rapid substitution of its original ligands by solvent (Eq. (5)) [7,8]. The intriguing outcome of this one-photon



photoredox process is the generation of three chemically distinct species: a cationic Lewis acid ( $\text{Co}^{2+}$ ), multiequivalents of an uncharged Lewis base ( $\text{NH}_3$ ), and a radical ( $\text{X}^{\bullet}$ ). Any one or combination of these species could initiate useful chemistry of a suitably functionalized substrate.

In 1987, we reported that the incorporation of  $[\text{Co}(\text{NH}_3)_5\text{Br}](\text{ClO}_4)_2$  into submicron films of poly[glycidyl methacrylate-co-ethyl acrylate] (abbreviated COP; Fig. 1), produces a photosensitive material that undergoes crosslinking upon exposure to deep-ultraviolet radiation and subsequent heating [9]. As shown in Fig. 2, the electronic absorption spectrum of a film is dominated by an intense band at 258 nm arising from a Br-to-Co charge transfer transition of the cobalt salt. Irradiation causes a steady bleaching of this band, consistent with the occurrence of a photoredox process that, in analogy to Eq. (5), generates one or more weakly-absorbing Co(II) species. While our results did not permit a detailed identification of the photoproducts in the film, we suggested that the reduced metal would remain

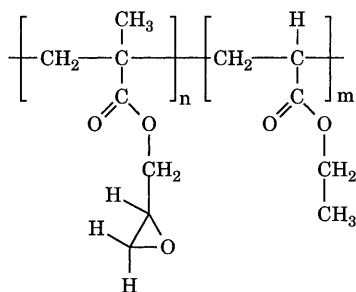


Fig. 1. Structure of the copolymer of glycidyl methacrylate and ethyl acrylate, COP. Value of  $n/m = 0.74$  for samples used in the cited studies.

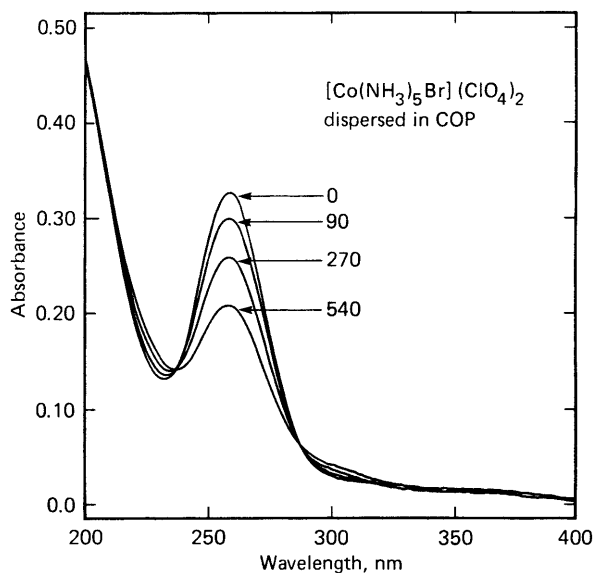


Fig. 2. Spectral changes observed upon 254-nm irradiation of a half-micron COP film containing  $[\text{Co}(\text{NH}_3)_5\text{Br}](\text{ClO}_4)_2$ . Indicated times are in seconds; to calculate exposure dose in  $\text{mJ cm}^{-2}$ , multiply time by 0.22. From reference [9]; reproduced by permission of The Electrochemical Society, Inc.

Table 1

Quantum yields for photoredox decomposition of cobalt(III) complexes in COP films exposed to 254 nm radiation

| Complex   | $\phi_{\text{Co}}^{2+}$ |
|---|-------------------------|
| $[\text{Co}(\text{NH}_3)_5\text{Br}](\text{ClO}_4)_2^{\text{a}}$            | $0.008 \pm 0.001$       |
| $[\text{Co}(\text{NH}_2\text{CH}_3)_5\text{Br}](\text{ClO}_4)_2^{\text{a}}$ | $0.007 \pm 0.002$       |
| $[\text{Co}(\text{NH}_2\text{CH}_3)_5\text{Cl}](\text{ClO}_4)_2^{\text{a}}$ | $0.012 \pm 0.004$       |
| $[\text{Co}(\text{NH}_3)_5\text{Br}](\text{BPh}_4)_2^{\text{b}}$            | $0.30 \pm 0.01$         |
| $[\text{Co}(\text{NH}_3)_6](\text{BPh}_4)_3^{\text{b}}$                     | $0.34 \pm 0.04$         |
| $[\text{Co}(\text{en})_3](\text{BPh}_4)_3^{\text{b}}$                       | $0.24 \pm 0.03$         |

<sup>a</sup> Data from reference [12].

<sup>b</sup> Data from reference [16].

coordinated to a number of  $\text{NH}_3$  ligands, since such complexes are known to exist in the solid state at room temperature. Dissociation of  $\text{NH}_3$  should occur, however, upon heating the polymer film.

Despite convincing evidence that  $[\text{Co}(\text{NH}_3)_5\text{Br}](\text{ClO}_4)_2$  undergoes photoredox decomposition in COP (Fig. 2), the irradiated polymer film dissolved completely in a 2-butanone/ethanol developer solution. In contrast, baking a film at 68–70°C for 6–7 min after an identical exposure rendered it insoluble in the developer. Since a control experiment revealed that heating alone does not cause insolubilization, we concluded that one or more of the products resulting from the photodecomposition of  $[\text{Co}(\text{NH}_3)_5\text{Br}](\text{ClO}_4)_2$  reacts with COP in a thermally-activated process. This reaction crosslinks the pendant epoxide groups on adjacent chains and thereby lowers the solubility of the polymer in the developer.

Identifying the photogenerated crosslinking agent posed an interesting mechanistic challenge, since, in principle, both the acidic  $\text{Co}^{2+}$  ion and the basis  $\text{NH}_3$  molecule can open the epoxide ring. To distinguish between these possibilities, we compared the photosensitivities of COP films containing  $[\text{Co}(\text{NH}_3)_5\text{Br}](\text{ClO}_4)_2$ ,  $[\text{Co}(\text{NH}_2\text{CH}_3)_5\text{Br}](\text{ClO}_4)_2$ , and  $[\text{Co}(\text{NH}_2\text{CH}_3)_5\text{Cl}](\text{ClO}_4)_2$  [10–12]. Like their amine counterpart, the methylamine complexes undergo photoredox decomposition in solution with the release of multiequivalents of base (Eq. (6)) [13]. While the analogous process occurs in COP films with similar quantum efficiency,  $\phi_{\text{Co}}^{2+}$ , for the three complexes (Table 1),  $\text{NH}_2\text{CH}_3$  is an appreciably stronger base than  $\text{NH}_3$ . Accordingly, we expected  $[\text{Co}(\text{NH}_2\text{CH}_3)_5\text{Br}](\text{ClO}_4)_2$  and  $[\text{Co}(\text{NH}_2\text{CH}_3)_5\text{Cl}](\text{ClO}_4)_2$  to be more effective as photoinitiators than  $[\text{Co}(\text{NH}_3)_5\text{Br}](\text{ClO}_4)_2$  if crosslinking of COP occurs via a base-mediated pathway, whereas the three complexes should yield roughly comparable results if crosslinking proceeds by way of  $\text{Co}^{2+}$  attack.

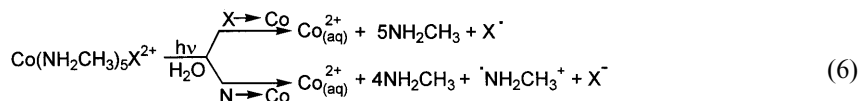
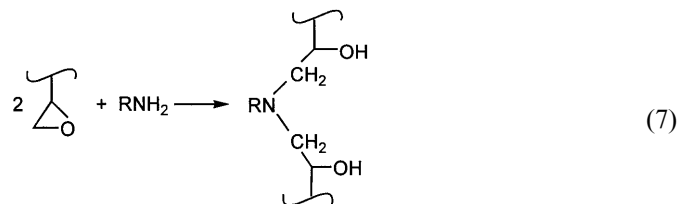


Figure 3 displays photosensitivity curves for COP films containing the three cobalt(III) complexes. The films were exposed to a graded series of doses of 254 nm radiation, heated at 70°C for 7 min, and then rinsed with a 2-butanone/ethanol developer solution. The normalized film thickness remaining after this treatment is plotted as a function of the logarithm of the radiation dose. Two features of these curves deserve special note. First, the films containing  $[\text{Co}(\text{NH}_2\text{CH}_3)_5\text{Br}](\text{ClO}_4)_2$  and  $[\text{Co}(\text{NH}_2\text{CH}_3)_5\text{Cl}](\text{ClO}_4)_2$  possess very similar photosensitivities. Second, and most importantly, these films are considerably more photosensitive than the film containing  $[\text{Co}(\text{NH}_3)_5\text{Br}](\text{ClO}_4)_2$ . These results establish that photoliberated base plays the key role in initiating the crosslinking of COP. A plausible mechanism for this process involves the nucleophilic attack of a(m)mine on the epoxides rings of neighboring polymer chains to form alcoholamine linkages (Eq. (7)).



Further support for this mechanism is provided by the contrasting behavior exhibited by a COP film containing *trans*- $[\text{Co}(\text{py})_4\text{Cl}_2]\text{Cl} \cdot 6\text{H}_2\text{O}$  (py is pyridine). While irradiation into a Cl-to-Co charge transfer band causes the expected redox decomposition of the complex in the film (Eq. (8)), subsequent heating does not initiate crosslinking of the polymer. This finding is consistent with the properties of pyridine, whose low base strength and lack of active hydrogens preclude it from attacking the epoxide ring via the pathway followed by  $\text{NH}_3$  and  $\text{NH}_2\text{CH}_3$ .

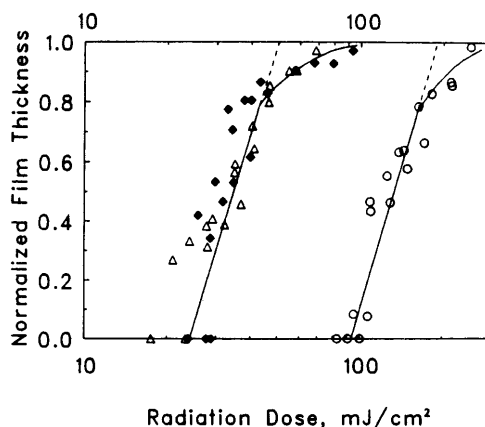


Fig. 3. Photosensitivity curves for films of COP containing  $[\text{Co}(\text{NH}_3)_5\text{Br}](\text{ClO}_4)_2$  ( $\circ$ ),  $[\text{Co}(\text{NH}_2\text{CH}_3)_5\text{Br}](\text{ClO}_4)_2$  ( $\blacklozenge$ ), or  $[\text{Co}(\text{NH}_2\text{CH}_3)_5\text{Cl}](\text{ClO}_4)_2$  ( $\triangle$ );  $\lambda_{\text{excit}} = 254 \text{ nm}$ . Reproduced with permission from reference [11].

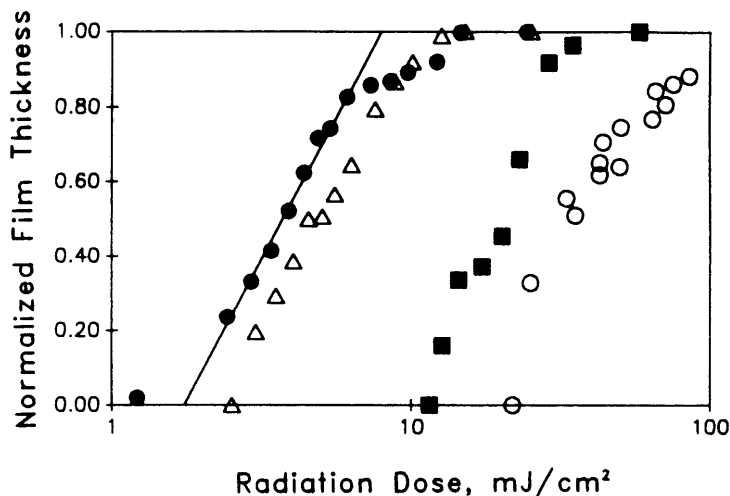
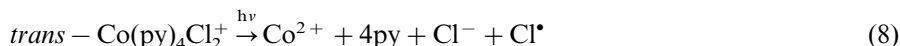
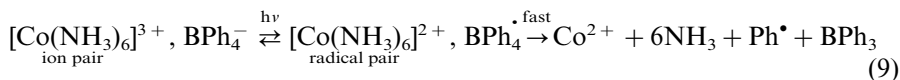


Fig. 4. Photosensitivity curves for films of COP containing  $[\text{Co}(\text{NH}_3)_6](\text{BPh}_4)_3$  (●),  $[\text{Co}(\text{NH}_3)_5\text{Br}](\text{BPh}_4)_2$  (△),  $[\text{Co}(\text{en})_3](\text{BPh}_4)_3$  (■), or  $[\text{Co}(\text{NH}_3)_5\text{Br}](\text{ClO}_4)_2$  (○);  $\lambda_{\text{excit}} = 254$  nm. Reproduced with permission from reference [16].



While the cobalt(III)–a(m)mine perchlorate complexes considered thus far satisfy several of the criteria for a practical photoinitiator, their low quantum efficiencies of photoredox decomposition in polymer films (Table 1) is problematic. This inefficiency most likely arises from rapid back-electron transfer between the primary photoproducts (e.g.  $\text{Co}(\text{NH}_3)_5^{2+}$  and  $\text{X}^\bullet$  in Eq. (5)) in the viscous polymer matrix. An attractive strategy for ameliorating this cage effect involves coupling the photoredox step with rapid secondary reactions that consume the photoproducts. For example, ultraviolet irradiation of  $[\text{Co}(\text{NH}_3)_6]^{3+}, \text{BPh}_4^-$  ( $\text{BPh}_4^-$  is tetraphenylborate anion) and related ion pairs in solution induces intermolecular electron transfer from  $\text{BPh}_4^-$  to its cobalt(III)–ammine partner (Eq. (9)) [14,15]. Both constituents of the resulting radical pair undergo rapid reactions that favor irreversible redox decomposition. Similar behavior in a COP film should increase both the quantum efficiency of base release and the resulting photosensitivity of the film toward crosslinking. To test this premise, we irradiated COP films containing



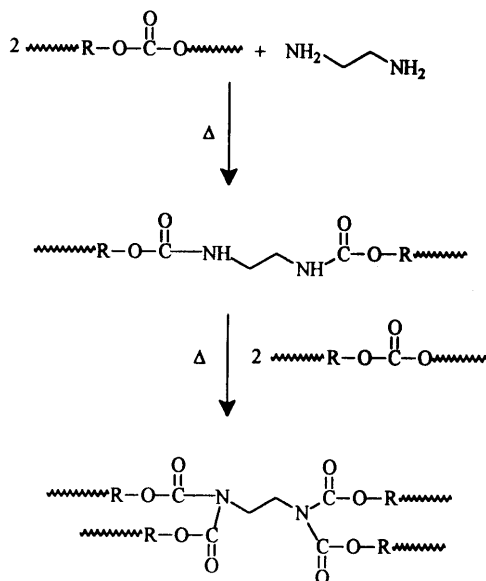
$[\text{Co}(\text{NH}_3)_6](\text{BPh}_4)_3$ ,  $[\text{Co}(\text{en})_3](\text{BPh}_4)_3$  (en is ethylenediamine), and  $[\text{Co}(\text{NH}_3)_5\text{Br}](\text{BPh}_4)_2$  [16]. Quantum yield data summarized in Table 1 show that all of the complexes undergo very efficient photoredox decomposition in the polymer. It should be noted that the effective quantum efficiency of base generation,  $\phi_{\text{base}}$ , equals  $\phi_{\text{Co}^{2+}}^{\text{2+}}$ , the quantum efficiency of decomposition, multiplied by the number of moles of released base; for  $[\text{Co}(\text{NH}_3)_6](\text{BPh}_4)_3$ ,  $\phi_{\text{base}} = 0.34 \times 6 = 2.0$ . As seen from

the photosensitivity curves in Fig. 4, this highly efficient release of base greatly reduces the radiation dose required to initiate crosslinking in COP films.

The photoinitiated chemistry that occurs in COP films containing a cobalt(III)–a(m)mine complex can be utilized for microimaging applications. Patterned irradiation causes release of a(m)mine (e.g. Eq. (9)) only in those areas of a film exposed to light, and subsequent heating produces the crosslinks (Eq. (7)) that render these areas insoluble. Rinsing the film with a developer solution dissolves the unexposed regions to yield a negative-tone relief image of the pattern. Using 254-nm radiation, we have achieved 1–2  $\mu\text{m}$  resolution via this approach [9–12,16].

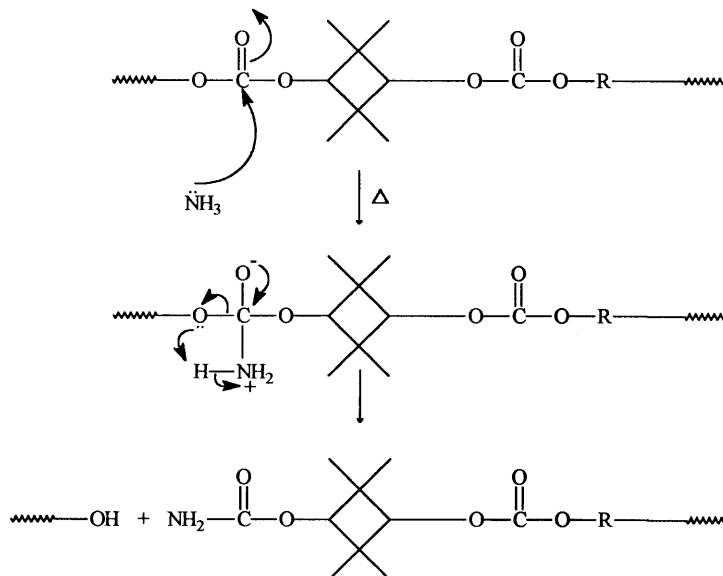
Aliphatic polycarbonates formed by the condensation copolymerization of the bischloroformate of 2,2,4,4-tetramethyl-1,3-cyclobutanediol with itself and with a variety of other diols possess a number of attractive physical properties including high molecular weight, low refractive index, high ultraviolet transparency, and good thermal behavior. Combining these polymers with base-generating photoinitiators has yielded an interesting new class of photoimagable materials [17]. Photoredox decomposition of  $[\text{Co}(\text{en})_3](\text{BPh}_4)_3$  in a polycarbonate film releases ethylenediamine that subsequently crosslinks the polymer via formation of bis(dicarbamate) linkages (Scheme 1). This chemistry insolubilizes the film in the exposed areas to yield negative-tone images. In an intriguing reversal of behavior, photochemical release of  $\text{NH}_3$  from  $[\text{Co}(\text{NH}_3)_6](\text{BPh}_4)_3$  leads to positive-tone images. While  $\text{NH}_3$  can form a carbamate via attack on the polycarbonate (Scheme 2), its weaker basicity disfavors further reaction to form the dicarbamate. Consequently, the predominant process is chain scission and eventual production of low molecular weight fragments that volatilize away at elevated temperatures.

In closing this section, we wish to call attention to the growing number of base-generating organic photoinitiators that have been developed in other laborato-



Scheme 1.



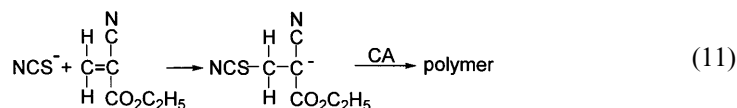
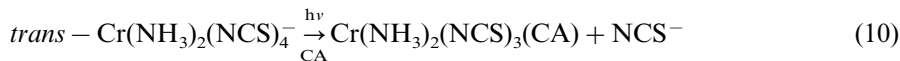


Scheme 2.

ries. Photochemical release of amines occurs from carbamates [18–20], *O*-acyloximes [21], oxime-urethane derivatives [22], and quarternary ammonium salts [23,24]. Several innovative applications of photogenerated bases also have been reported [25–28].

### 3. Anion-generating photoinitiators

Relatively little attention has been accorded to photoinitiators that generate anions. Our entry into this area occurred in 1991, when we reported that irradiation of *trans*-Cr(NH<sub>3</sub>)<sub>2</sub>(NCS)<sub>4</sub><sup>−</sup> dissolved in neat ethyl  $\alpha$ -cyanoacrylate monomer (abbreviated CA) initiates rapid anionic polymerization [29]. In the initial step of this process, the metal complex undergoes photochemical release of NCS<sup>−</sup> from a ligand field excited state (Eq. (10)) [30,31]. Attack of NCS<sup>−</sup> on the carbon–carbon double bond of the electrophilic monomer yields a resonance-stabilized carbanion, from which polymerization propagates rapidly via repetitive addition of CA units to the active anionic site (Eq. (11)).



Rates of photoinitiated polymerization were determined for CA solutions of *trans*-Cr(NH<sub>3</sub>)<sub>2</sub>(NCS)<sub>4</sub><sup>−</sup> by real-time Fourier transform infrared spectroscopy. The short sampling time and sensitivity to molecular structure of this technique allow the rapid and accurate measurement of monomer concentration during irradiation [32]. The extent of polymerization in a sample is defined by Eq. (12), where  $A_o$  denotes the

$$\% \text{ polymerization} = \frac{(A_o - A_t)}{A_o} \times 100 \quad (12)$$

initial (dark) integrated absorbance of the C=C stretching band of CA at 1616 cm<sup>−1</sup>, and  $A_t$  is the integrated absorbance after irradiation for time  $t$ . As seen in Fig. 5, polymerization commences within the first few seconds following exposure to light and reaches a plateau within 10–15 s at the highest photoinitiator concentration. The rate of photoinitiated polymerization,  $R_p$ , can be calculated from Eq. (13), where  $A_{t_1}$  and  $A_{t_2}$  represent the integrated absorbances of the 1616 cm<sup>−1</sup> band at the indicated times, and  $M$  is the molar concentration of vinyl groups in CA. Maximum rates of 3.0, 1.3 and 0.60 M s<sup>−1</sup> result for CA samples containing  $2.0 \times 10^{-3}$ ,  $5.4 \times 10^{-4}$ , and

$$R_p = \frac{M(A_{t_1} - A_{t_2})}{A_o(t_2 - t_1)} \quad (13)$$

$2.2 \times 10^{-4}$  M concentrations of *trans*-Cr(NH<sub>3</sub>)<sub>2</sub>(NCS)<sub>4</sub><sup>−</sup>, respectively. The trend toward faster rates at higher photoinitiator concentrations reflects the greater

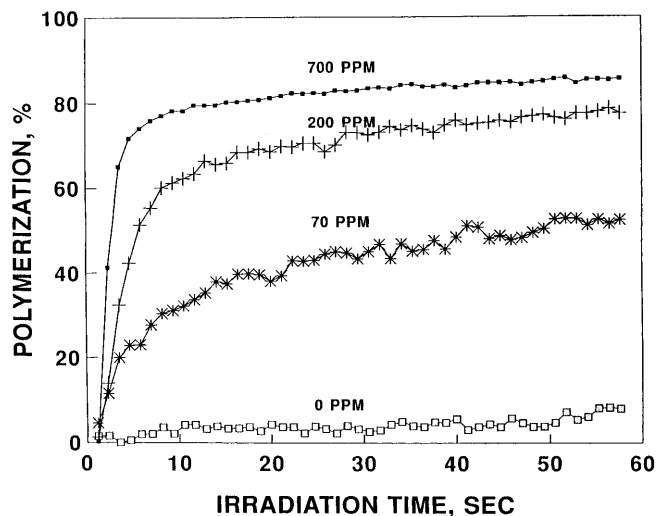


Fig. 5. Plots of percentage polymerization versus time of irradiation for samples of CA containing the indicated amounts of *trans*-Cr(NH<sub>3</sub>)<sub>2</sub>(NCS)<sub>4</sub><sup>−</sup> (700 ppm =  $2.0 \times 10^{-3}$  M). Thin films of these samples were coated onto acid-treated silicon wafers and irradiated with a 500 mW cm<sup>−2</sup> polychromatic (254–630 nm) light source. Reproduced from reference [29]. Copyright 1991 American Chemical Society.

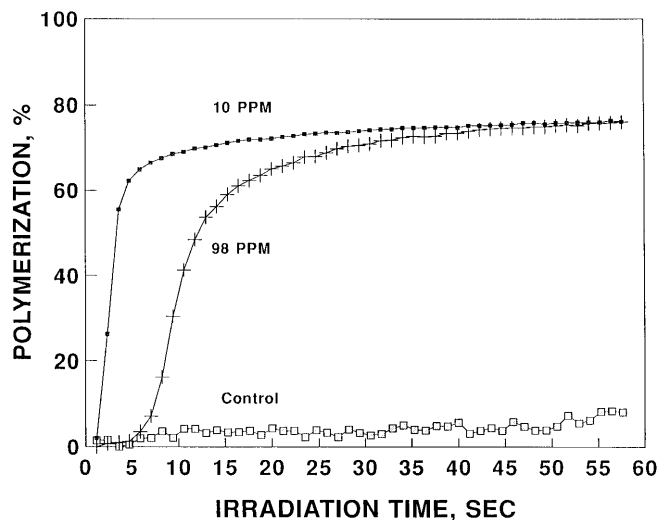
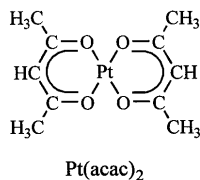


Fig. 6. Plots of percentage polymerization vs time of irradiation for samples of CA containing  $2.0 \times 10^{-3}$  M *trans*-Cr(NH<sub>3</sub>)<sub>2</sub>(NCS)<sub>4</sub><sup>−</sup> and the indicated amounts of methanesulfonic acid. Control sample contained no photoinitiator and 10 ppm of the acid.

fraction of light absorbed by the sample and the corresponding increase in the concentration of the photogenerated species responsible for initiating polymerization.

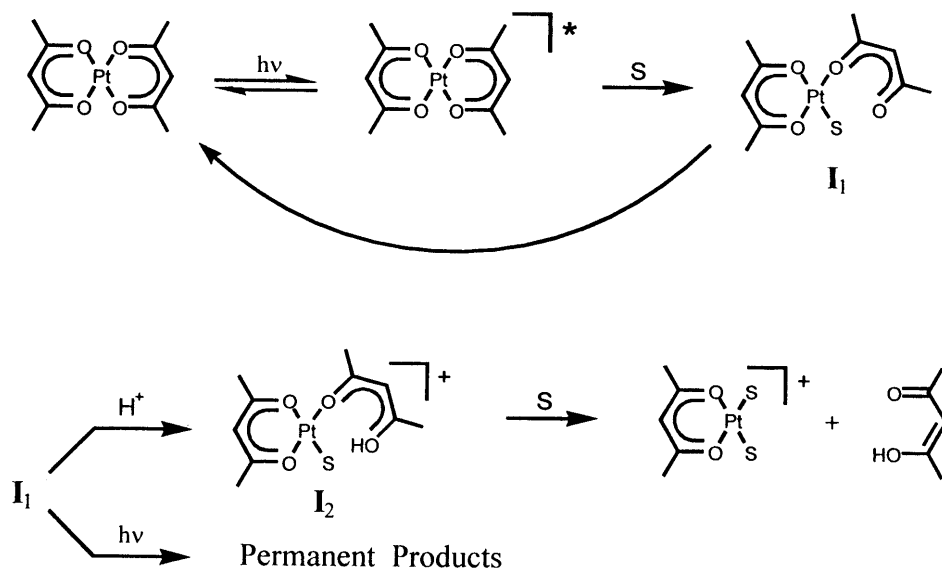
The key role played by anionic species in the polymerization of CA is underscored by the marked inhibition that occurs in the presence of methanesulfonic acid. As illustrated in Fig. 6, increasing the acid concentration from 10 to 98 ppm in the monomer sample introduces an induction period and lowers the polymerization rate. This inhibition by strong acid reflects the ability of protons to scavenge photogenerated NCS<sup>−</sup> and/or anionic sites on the growing polymer chain.

Our search for new anionic photoinitiators led us to investigate Pt(acac)<sub>2</sub> (structure shown below; acac<sup>−</sup> is the acetylacetonate anion) [33]. This uncharged, d<sup>8</sup> square-planar β-diketonate complex readily dissolves in a range of nonaqueous solvents, exhibits excellent thermal stability in solution, and absorbs strongly in the ultraviolet region. We reasoned that photoexcitation of the complex to a ligand field or a ligand-to-metal charge transfer excited state should weaken the Pt–O bonds and thereby facilitate the production of acac<sup>−</sup>. Initial experiments revealed that Pt(acac)<sub>2</sub> indeed functions as a highly effective photoinitiator for the anionic polymerization of CA.



Detailed studies of the solution photochemistry of  $\text{Pt}(\text{acac})_2$  led to the proposed mechanism in Scheme 3 [34]. Irradiation of the complex populates a reactive excited state (denoted by an asterisk) that can undergo relaxation to the ground state in competition with heterolytic cleavage of a Pt–O bond to form intermediate  $\text{I}_1$ . We have identified  $\text{I}_1$  as a Pt(II) complex containing a monodentate O-bonded  $\text{acac}^-$  ligand and a coordinated solvent molecule, S. The fate of  $\text{I}_1$  depends upon the solvent and the extent of reaction. The dominant pathway in  $\text{CH}_3\text{CN}$  at low photochemical conversions is rechelation of the dangling  $\text{acac}^-$  ligand to regenerate  $\text{Pt}(\text{acac})_2$ . At higher conversions, inefficient secondary photolysis of  $\text{I}_1$  affords a complicated mixture of products that includes  $\text{Pt}(\text{acac})(\text{CH}_3\text{CN})_2^+$ ,  $\text{H}(\text{acac})$ , and oligomeric species containing Pt(acac) units. Rapid protonation of  $\text{I}_1$  in the presence of acid generates  $\text{I}_2$ , a species containing a monodentate-bound enol tautomer of acetylacetone. The added proton reduces the basicity of this ligand and thereby facilitates thermal release of  $\text{H}(\text{acac})$  to yield  $\text{Pt}(\text{acac})(\text{CH}_3\text{CN})_2^+$ . In neat CA,  $\text{I}_1$  can serve as a latent source of  $\text{acac}^-$ . In a process analogous to protonation, electrophilic attack of CA on the dangling end of the monodentate  $\text{acac}^-$  ligand can produce the carbanion (refer to Eq. (11)) that propagates anionic polymerization.

Recently, we reported the first examples of anionic photoinitiation involving members of the ferrocene family, **I–III** [35]. These metallocene complexes are easily synthesized, relatively inexpensive, soluble in a wide range of nonaqueous solvents, and thermally stable in solution. The parent complex,  $\text{Fe}(\eta^5\text{-C}_5\text{H}_5)_2$ , displays two relatively weak bands above 300 nm attributable to ligand field transitions. In



Scheme 3.

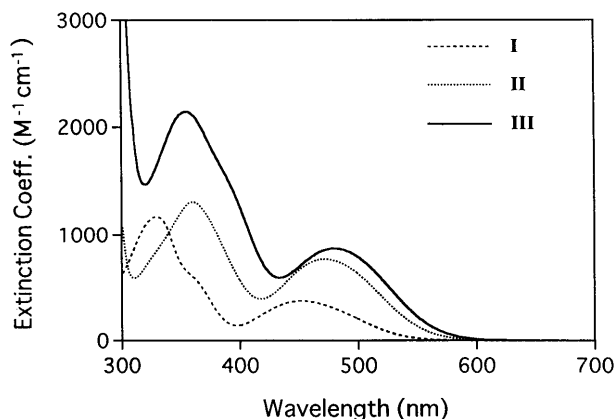
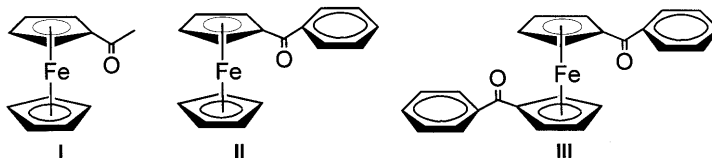


Fig. 7. Electronic absorption spectra of **I–III** in room-temperature ethyl  $\alpha$ -cyanopropionate. Reproduced from reference [35]. Copyright 1998 American Chemical Society.

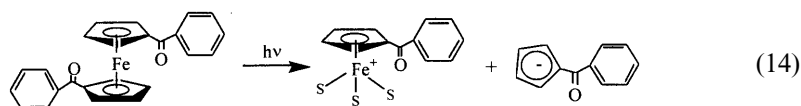
contrast, both bands in the acyl-functionalized derivatives appear at longer wavelengths and with significantly higher intensities (Fig. 7). These differences arise from conjugation of the cyclopentadienide ring  $\pi$ -orbitals with the  $\pi$  orbitals of the adjacent carbonyl group in the photoexcited complex [36,37]. This interaction introduces a degree of charge transfer into the electronic transitions, resulting in a stabilization of the excited states populated and an enhanced transition probability.



Data compiled in Table 2 reveal that **I–III** function as photoinitiators for the polymerization of CA. 1,1'-Dibenzoylferrocene, **III**, is particularly effective in this role, even at wavelengths well into the visible region. The nature of the active initiating species was probed in a series of scavenging experiments. Initiation by photogenerated radicals appears to be unlikely, since the addition of 0.029 M hydroquinone, a common radical scavenger, to CA solutions containing **III** did not affect the rate of photoinitiated polymerization. In contrast, adding 0.001 M methanesulfonic acid to these solutions retarded polymerization. As noted earlier, such behavior is diagnostic of initiation by an anionic species that can be scavenged by protons.

Disappearance quantum yield ( $\phi_{\text{dis}}$ ) data summarized in Table 3 demonstrate that **II** and **III** undergo efficient photochemistry in solution. Analysis of the photoproducts by mass spectrometry revealed that the primary photoprocess is ring-metal cleavage to yield a benzoyl-functionalized cyclopentadienide carbanion and the corresponding half-sandwich iron(II) complex (shown for **III** in Eq. (14); S is solvent) [37]. This carbanion, which should be rapidly scavenged by protons, can

serve as the initiating species in the polymerization of CA. The effectiveness of **III** as a photoinitiator (Table 2) most likely arises from a high quantum efficiency for carbanion formation (Table 3).



These results demonstrate that 1,1'-dibenzoyl-functionalized ferrocenes comprise an attractive new class of anionic photoinitiators. Photogeneration of a carbanion by these complexes should prove to be useful for initiating the reactions of a variety of substrates. Additional studies of the photoinitiation properties of **III** and several

Table 2  
Studies of I–III as photoinitiators for the polymerization of CA<sup>a</sup>

| Photoinitiator (PI) | PI concentration mol/l $\times 10^3$ (ppm) | $\lambda_{\text{ex}}$ (nm) | Photopolym. time <sup>b</sup> (s) |
|---------------------|--|----------------------------|-----------------------------------|
| I                   | 1.89 (404)                                 | > 290                      | 552                               |
| II                  | 1.46 (404)                                 | > 290                      | 176                               |
| II                  | 1.90 (523)                                 | 436 <sup>c</sup>           | > 900                             |
| III                 | 1.07 (403)                                 | > 290                      | 3.1                               |
| III                 | 1.61 (605)                                 | 436 <sup>c</sup>           | 38                                |
| III                 | 2.40 (902)                                 | 546 <sup>d</sup>           | 31                                |

<sup>a</sup> Reproduced from reference [35]. Copyright 1998 American Chemical Society. General conditions: a 2 ml sample of CA containing the indicated concentration of photoinitiator was irradiated with stirring in a 1 cm rectangular plastic (methacrylate) cell. The excitation source was a 200-W high pressure mercury lamp. No attempt was made to exclude air from the sample.

<sup>b</sup> Irradiation time required for the sample to become so viscous that the 8-mm stirring bar ceased to spin.

<sup>c</sup> Sample absorbance = 1.0; light intensity =  $7.8 \times 10^{-8}$  einstein  $\text{s}^{-1}$ .

<sup>d</sup> Sample absorbance = 0.7; light intensity =  $1.2 \times 10^{-7}$  einstein  $\text{s}^{-1}$ .

Table 3  
Disappearance quantum yield ( $\phi_{\text{dis}}$ ) data for II and III

| Complex <sup>a</sup> | Solvent            | $\phi_{\text{dis}}$ <sup>b</sup> |
|----------------------|--------------------|----------------------------------|
| II                   | CH <sub>3</sub> OH | 0.083                            |
| II                   | CP <sup>c</sup>    | 0.035                            |
| III                  | CH <sub>3</sub> OH | 0.45                             |
| III <sup>d</sup>     | CH <sub>3</sub> OH | $0.42 \pm 0.06$                  |
| III                  | CP <sup>c</sup>    | 0.28                             |

<sup>a</sup> Experimental conditions: excitation wavelength, 546 nm; light intensity,  $1.1 \pm 0.1 \times 10^{-7}$  einstein  $\text{s}^{-1}$ ; temperature,  $22 \pm 1^\circ\text{C}$ .

<sup>b</sup> Where quoted, error limit represents mean deviation of two runs; estimated accuracy of  $\phi_{\text{dis}}$  is 10–15%.

<sup>c</sup> CP is ethyl  $\alpha$ -cyanopropionate.

<sup>d</sup> Purged by argon bubbling for 30 min prior to irradiation.

analogues containing substituents on the phenyl rings will be described in future reports.

#### 4. Concluding remarks

This article has reviewed the status of our ongoing search for novel inorganic and organometallic photoinitiators. Results to date have expanded the range of available photoinitiators beyond the traditional radical- and acid-releasing systems to systems that generate uncharged Lewis bases and anions. The knowledge gained from such studies has enhanced our fundamental understanding of the thermal and photochemical reactions involved in the photoinitiation process. Equally important, this knowledge has afforded a basis for the rational design of the next-generation photoinitiators required to satisfy the increasingly demanding needs of industry for advanced photosensitive materials. Given this economic impetus, the search for new and more effective photoinitiators should continue to be an active research area over the next several years.

#### Acknowledgements

The author thanks his many talented coworkers, whose names appear in the references, for their valuable contributions to the studies conducted in his laboratory. Financial support for this work was received from the National Science Foundation, IBM Corporation, and JSR Corporation.

#### References

- [1] S.P. Pappas (Ed.), *Radiation Curing: Science and Technology*, Plenum Press, New York, 1992.
- [2] A.B. Scranton, C.N. Bowman, R.W. Peiffer (Eds.), *Photopolymerization: Fundamentals and Applications*, ACS Symposium Series, no. 673, American Chemical Society, Washington, DC, 1997.
- [3] E. Reichmanis, F.M. Houlihan, O. Nalamasu, T.X. Neenan, *Chem. Mater.* 3 (1991) 394.
- [4] D.B. Yang, C. Kutal, in: S.P. Pappas (Ed.), *Radiation Curing: Science and Technology*, ch. 2, Plenum, New York, 1992.
- [5] B.M. Monroe, G.C. Weed, *Chem. Rev.* 93 (1993) 435.
- [6] R.S. Davidson, *J. Photochem. Photobiol. A: Chem.* 73 (1993) 81.
- [7] V. Balzani, V. Carassiti, *Photochemistry of Coordination Compounds*, ch. 11, Academic Press, London, 1970.
- [8] J.F. Endicott, in: A.W. Adamson, P.D. Fleischauer (Eds.), *Concepts of Inorganic Photochemistry*, ch. 3, Wiley-Interscience, New York, 1975.
- [9] C. Kutal, C.G. Willson, *J. Electrochem. Soc.* 134 (1987) 2280.
- [10] C. Kutal, S.K. Weit, S.A. MacDonald, C.G. Willson, *J. Coat. Technol.* 62 (1990) 63.
- [11] C. Kutal, S.K. Weit, R.D. Allen, S.A. MacDonald, C.G. Willson, in: *Advances in Resist Technology and Processing VIII*, Proc. SPIE, 1466, 1991, pp. 362.
- [12] S.K. Weit, C. Kutal, R.D. Allen, *Chem. Mater.* 4 (1992) 453.
- [13] S.K. Weit, G. Ferraudi, P.A. Grutsch, C. Kutal, *Coord. Chem. Rev.* 128 (1993) 225.
- [14] H. Hennig, D. Walther, P. Thomas, *Z. Chem.* 23 (1983) 446.

- [15] Z. Wang, C. Kotal, *Inorg. Chim. Acta* 226 (1994) 285.
- [16] C. Kotal, B.J. Palmer, Z. Wang, in: *Advances in Resist Technology and Processing XII*, Proc. SPIE, 2438, 1995, pp. 795.
- [17] J.D. Davies, W.H. Daly, Z. Wang, C. Kotal, *Chem. Mater.* 8 (1996) 850.
- [18] J.F. Cameron, J.M.J. Frechet, *J. Am. Chem. Soc.* 113 (1991) 4303.
- [19] A. Mochizuki, T. Teranishi, M. Ueda, *Macromolecules* 28 (1995) 365.
- [20] J.F. Cameron, C.G. Willson, J.M.J. Frechet, *J. Am. Chem. Soc.* 118 (1996) 12925.
- [21] K. Ito, Y. Shigeru, Y. Kawata, K. Ito, M. Tsunooka, *Can. J. Chem.* 73 (1995) 1924.
- [22] K.H. Chae, *Macromol. Rapid Commun.* 19 (1998) 1.
- [23] S. Hassoon, A. Sarker, M.A.J. Rodgers, D.C. Neckers, *J. Am. Chem. Soc.* 117 (1995) 11369.
- [24] J.E. Hanson, K.H. Jensen, N. Gargiulo, D. Motta, D.A. Pingor, A.E. Novembre, D.A. Mixon, J.M. Kometani, C. Knurek, in: E. Reichmanis, C.K. Ober, S.A. MacDonald, T. Iwayanagi, T. Nishikubo (Eds.), *Microelectronics Technology: Polymers for Advanced Imaging and Packaging*, ch. 9, ACS Symposium Series, No. 614, American Chemical Society, Washington, DC, 1995.
- [25] K.A. Graziano, S.D. Thompson, M.R. Winkle, *Proc. SPIE* 1466 (1991) 75.
- [26] D.R. McKean, G.M. Wallraff, W. Volksen, N.P. Hacker, M.I. Sanchez, J.W. Labadie, in: L.F. Thompson, C.G. Willson, S. Tagawa (Eds.), *Polymers for Microelectronics*, ch. 28, ACS Symposium Series, No. 537, American Chemical Society, Washington, DC, 1994.
- [27] A. Mejiritski, A.M. Sarker, B. Wheaton, D.C. Neckers, *Chem. Mater.* 9 (1997) 1488.
- [28] J.M.J. Frechet, M. Leung, E.J. Urankar, C.G. Willson, J.F. Cameron, S.A. MacDonald, C.P. Niesert, *Chem. Mater.* 9 (1997) 2887.
- [29] C. Kotal, P.A. Grutsch, D.B. Yang, *Macromolecules* 24 (1991) 6872.
- [30] E.E. Wegner, A.W. Adamson, *J. Am. Chem. Soc.* 88 (1966) 394.
- [31] M. Cusumano, C.H. Langford, *Inorg. Chem.* 17 (1978) 2222.
- [32] D.B. Yang, *J. Polym. Sci. Part A* 31 (1993) 199.
- [33] B.J. Palmer, C. Kotal, R. Billing, H. Hennig, *Macromolecules* 28 (1995) 1328.
- [34] R.J. Lavallee, B.J. Palmer, R. Billing, H. Hennig, G. Ferraudi, C. Kotal, *Inorg. Chem.* 36 (1997) 5552.
- [35] Y. Yamaguchi, B.J. Palmer, C. Kotal, T. Wakamatsu, D.B. Yang, *Macromolecules* 31 (1998) 5155.
- [36] A.M. Tarr, D.M. Wiles, *Can. J. Chem.* 46 (1968) 2725.
- [37] Y. Yamaguchi, C. Kotal, *Inorg. Chem.* 38 (1999) 4861.